ECCOMAS Congress 2016
VII European Congress on Computational Methods in Applied Sciences and Engineering
Yuji Kobayashi, Kenji Yoshida, Itsuhei Kohri, Masaharu Sakai and Hideo Asano
Crete Island, Greece, 5–10 June 2016

LARGE-SCALE LES ANALYSIS OF AUTOMOTIVE ENGINE COOLING FAN

Yuji Kobayashi[1], Kenji Yoshida[2], Itsuhei Kohri[1], Masaharu Sakai[2], Hideo Asano[2]

[1] Tokyo City University
1-28-1, Tamazutsumi, Setagaya, Tokyo, 158-0087, Japan
e-mail: {yujikoba, ikohri}@tcu.ac.jp

[2] DENSO CORPORATION
1-1 Syouwacho, Kariya, Aichi, 448-8661, Japan
e-mail: {KENJI_K_YOSHIDA, MASAHARU_SAKAI, HIDEO_ASANO}@denso.co.jp

Keywords: Engine cooling fan; Computational Fluid Dynamics (CFD); Large Eddy Simulation (LES)

Abstract. *The purpose of this study is to develop a more efficient engine cooling fan with low noise by understanding the detail of flow structures around the fan. As in the first report, this study focused on the P–Q characteristic and revealed the typical flow structures primary influencing the performance of a ring fan using large-scale LES analysis with HPCS (high-performance computer systems) after experimental validation.*

1 INTRODUCTION

In recent years, there has been a trend to develop a smaller engine cooling fan because of reduced space of the engine compartment due to expansion of the cabin space. Since the P–Q (pressure gain–flow rate) characteristic, which determines the engine cooling performance, varies with the square of the diameter and the number of revolutions of the fan, the performance degradation should be minimized when downsizing. It was shown that a similar cooling performance can be attained by adopting an equal total surface area of the blade using a homothetic design with short cord length and increasing the number of blades under the region of high flow rate (low pressure loss) [1]. However, simply increasing the number of revolutions and/or the number of blades to improve the cooling performance will result in high aerodynamic noise and/or cacophony of the cooling fan. Therefore, the development of a high-performance but low-noise small fan is urgently required. To achieve a significant improvement, it is necessary to understand the relationship between the fan performance and the flow structures around the fan. Many CFD analyses have been conducted to analyse actual phenomena that are difficult to reproduce via experiment [2, 3]. Basically, P–Q characteristic is steady, so it can be calculated using steady state CFD simulation like what other authors conducted [4, 5]. Moreover, it is also important to clarify the relation between the fan performance and the flow structures in each frequency when we consider the aerodynamic noise to

attain a major improvement. However, a successful research concerning this has not been reported yet.

Considering the above background, this research aims to clarify the mechanism of the generated aerodynamic noise of the cooling fan by associating the flow structures with the source point of the turbulence and the Blade Passing Frequency (BPF) noise. As a first step of the research, the detail of the flow structures around the fan was determined by large eddy simulation (LES) analysis using high-performance computing systems (HPCS) of K computer and FX-10 super computing systems. In particular, three kinds of grid and time scale, i.e., small-, middle-, and large-scale LES analyses were conducted to reveal the dominant flow structures on the performance and the essential information for the accurate prediction after experimental validations.

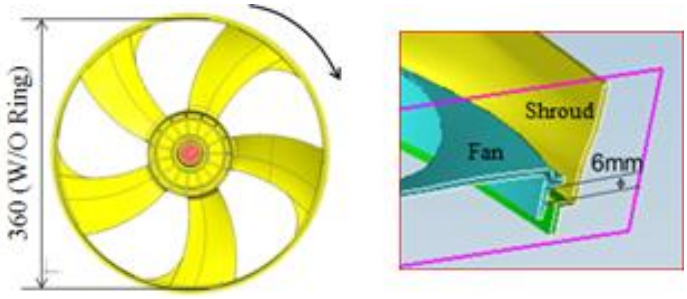

Figure 1: Test piece used in present study

2 METHODOLOGY

2.1 Experimental method

This study used a ring fan as a test piece as shown in Fig.1. The fan has five even-pitched blades with a ring at the tip of the blade. It is a real scale model of an actual engine cooling fan, which has a diameter of 360 mm. The performance of the fan was examined by measuring the flow rate and pressure gain at 2080 rpm in a test chamber. A shroud was only installed as peripheral equipment, and the clearance between outer wall of the ring and inner wall of the shroud was set at 6 mm. The experimental uncertainty of the measurement of the performance of the fan has been calculated to be within ±1%. In this study, the Reynolds number *Re* was approximately 9.4×10^5, based on the tip velocity (39.2 m/s) and diameter of the fan (360 mm).

In addition, the spectrum of the velocity magnitude measured by I type hot-wire 10 mm behind the trailing edge of the fan was calculated using fast Fourier transform (FFT) analysis for the experimental validation of the unsteady amount

2.2 CFD setup

Fig.2 shows the computational model and grid used in this study. Three types of computational models with difference in grid and time resolution were used. For small-scale analysis, tetrahedral unstructured grids were adopted in the entire computational domain, and the minimum size of the grid at the blade surface was 0.5 mm. Thus, the total number of elements was approximately 14 million for this model. On the other hand, for middle-scale analysis, hexahedral grids were adopted in the entire computational domain, and the minimum size of the grid at the blade surface was 0.1 mm. Hence, the total number of elements was approximately 86 million. For large-scale analysis, the grid resolution was doubled in each coordinate

compared to the middle-scale model. Consequently, the total number of elements was approximately 690 million. The finite element method was adopted to solve the unsteady LES using low-Mach-number approximation. The dynamic Smagorinsky model (DSM) for the sub-grid-scale (SGS) model and the Crank–Nicolson method for time discretization were used. The overset method [6] was used for the space around the rotating blade. The calculation code for the FrontFlow/blue-Ver.8.1 was used in this study. Time step size was set to 7.67×10^{-6} s for the small- and middle-scale analyses and 3.83×10^{-6} s for the large-scale analysis to ensure that the Courant number is less than one in all elements. Table 1 summarizes the main features of the computational method and simulation parameters.

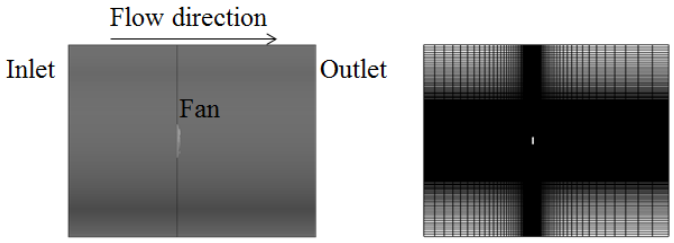

(a) Computational Domain and grid at section of the centre plane

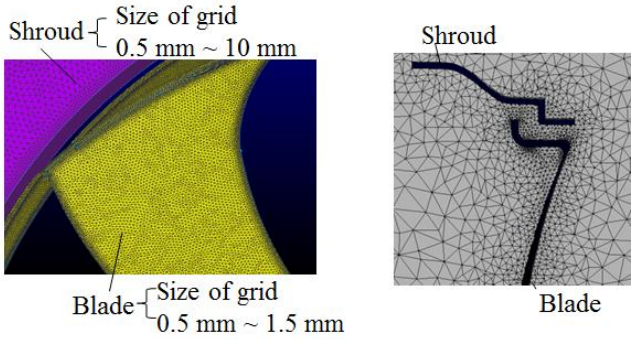

(b) Computational grid used for small-scale analysis

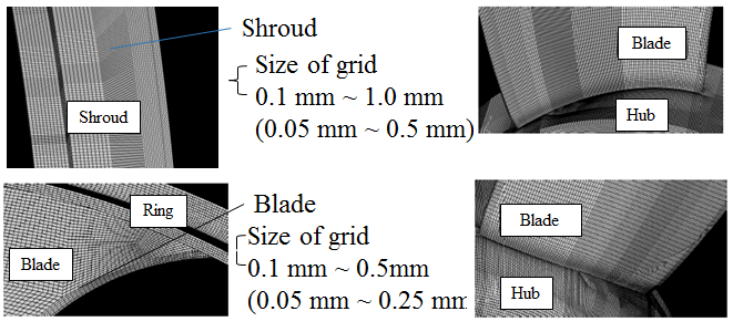

(c) Computational grid used for middle- and large-scale analyses; w/o brackets: middle-scale, with brackets: large-scale

Figure 2: Computational model and grid used in this study

	Small-scale	Middle-scale	Large-scale
Governing Equation	NS Equations		
	Continuity Equation		
Fluid	Incompressible		
State	Unsteady		
Turbulence Model	LES (DSM)		
Treatment of Rotation	Overset method		
Time discretization	Crank-Nicolson		
Cell Structure	All Tetrahedral	All Hexahedral	
Total Number of Cells	14.0 Million	86.0 Million	690 Million
Time Step [s]	7.67×10^{-6}		3.83×10^{-6}

Table 1: Specifications for fan calculations

3 VALIDATION OF COMPUTATIONAL ACCURACY

The fan performance was evaluated using the $\varphi - \psi^*$ characteristics, where φ and ψ^* are the coefficients of the flow rate and pressure gain, respectively, as defined by the following formulas:

$$\varphi = \frac{Q}{u_t \cdot A} \tag{1}$$

$$\psi^* = \frac{2\Delta P}{\rho \cdot u_t^{\,2}} \tag{2}$$

where Q, A, u_t, ρ, and ΔP denote the flow rate, frontal area of the rotating region of the fan, tip velocity, air density, and pressure difference between the inside and the outside of the chamber, respectively.

Fig.3 shows the $\varphi - \psi^*$ performance obtained by calculation compared with the experimental results. Here, $\varphi = 0.1$ means the working condition and this study focused only on that condition. The numbers in Fig.3 indicate the ratio of the CFD result to the experimental result. As shown, the proportion is 82.5% for small-scale and 121.0% for middle-scale; therefore, the predictive accuracy is not good. On the other hand, large-scale result shows good agreement with the experimental value as the proportion is 99.0%. Finally, Fig.4 shows the velocity spectrum of the wake obtained by middle-scale calculation compared with the experimental result at the point 10 mm behind the trailing edge and for 170 mm radius of the fan. The result of the simulation also shows good agreement with the experimental value in the qualitative manner.

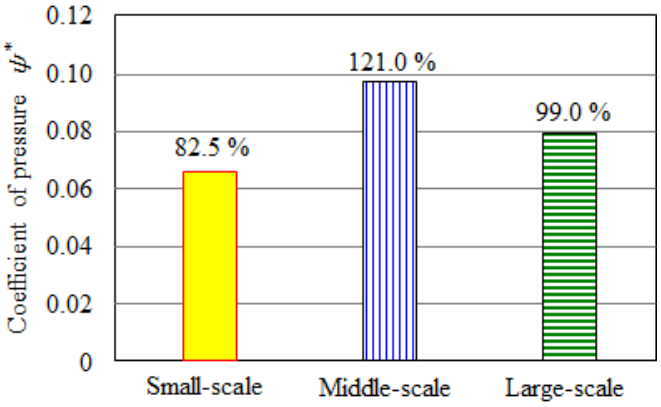

Figure 3: ψ^* characteristic calculated at the condition in $\varphi = 0.1$

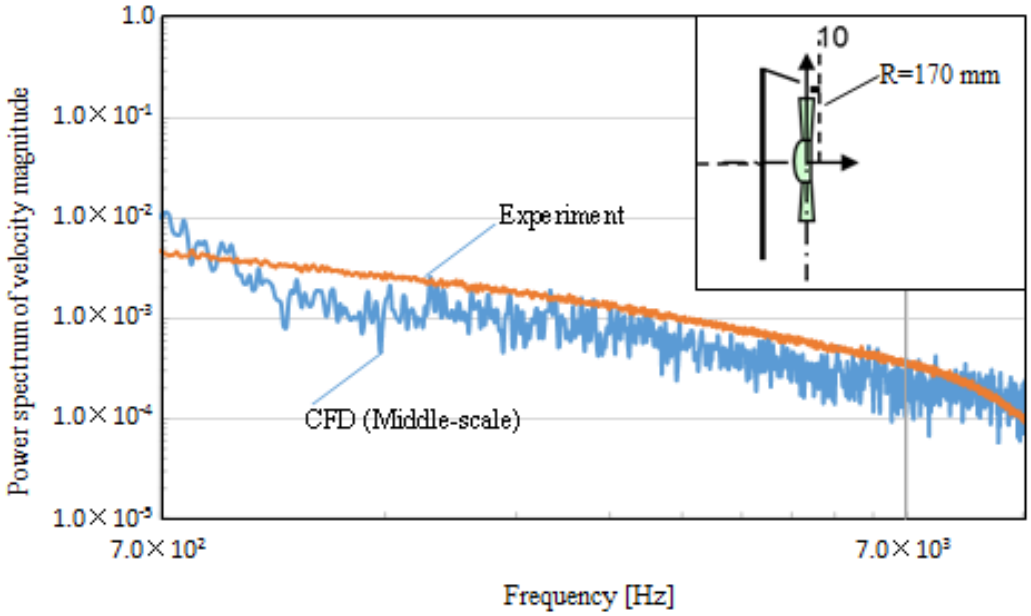

Figure 4: Power spectrum of velocity magnitude of wake flow

4 RELATION BETWEEN PERFORMANCE AND FLOW STRUCTURES

In this section, the essential point to the predictive accuracy is determined by comparing the flow structures of three kinds of simulations. Then, the relationship between the flow structures and the fan performance is discussed. Fig.5 shows the coefficient of pressure C_p of root mean square (RMS) value distribution, which denotes the time variation, while Fig.6 shows C_p distribution on the blade surface as defined by the following formula:

$$C_p = 2p/\left(\rho \cdot u_t^{\,2}\right) \tag{3}$$

Here, p denotes the local static pressure. It was found that the pressure fluctuation occurred locally at the suction surface of the leading edge and/or at the pressure surface of the leading edge near the tip for middle- and large-scale analyses. In contrast, the distribution feature was different particularly on the suction surface for small-scale analysis. This behaviour was also

confirmed by C_p distribution in perspective and the detail information was verified by C_p profile of concentric section of the blade surface at radius R = 110 and 150 mm as shown in Fig.7. Firstly, by comparing small-scale against middle- and large-scale, pressure recovery on the suction surface indicated different features. In addition, from the C_p profile of R = 150 mm at the leading edge, the prediction with small-scale of the attack angle of flow shows a large difference compared with the others. Next, by comparing middle- against large-scale, the difference of C_p was confined to the immediate vicinity of leading edge. This means that the difference of the $\varphi-\psi^*$ characteristic between middle- and large-scale was primarily caused by the flow structures between the blades (spatial flow structures). To confirm this theory, spatial vortex structures represented by isosurface of velocity gradient tensor of the second invariance Q were visualized as shown in Fig.8. As a result, for middle- and large-scale, it was observed that the turbulent vortex structures were generated from the leading and trailing edges. On the other hand, the vortex structures for small-scale were generated only at the leading edge, which corresponds to a separation vortex. It should be noted that the grid resolution was too poor to calculate the flow in boundary layer and/or turbulent wake structures. To clarify the influence of these turbulent structures on the spatial flow field around the fan, Q distribution and distribution of coefficient of velocity magnitude C_v normalized by tip velocity u_t at the section of R = 110 and 150 mm are shown in Fig.9 and Fig.10. For middle-scale analysis, it was found that the attack angle of flow was higher than large-scale because a larger turbulent structure was generated at the leading edge. In contrast, turbulent structures near the blade surface and wake for middle-scale were smaller than large-scale. Consequently, it should be noted that the attack angle of flow varied due to the difference of wake structures and finally changed the flow structures between the blades. This means that the essential point for the accurate prediction is the attack angle of flow in case of a ring fan because there is no large tip vortex that is always generated in case of a propeller fan. In other words, the flow in boundary layer and wake structures, which determines the flow field between the blades, dominates the performance of a ring fan. On the other hand, in a propeller fan used in previous studies [4], the essential point for the accurate prediction is the resolution of the spatial tip vortex because the vortex dominates the fan performance.

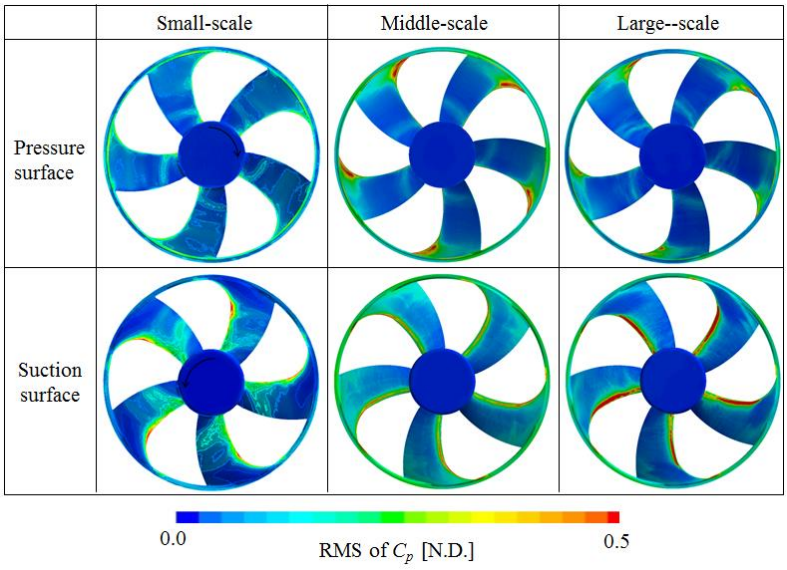

Figure 5: RMS distribution of C_p on the blade surface

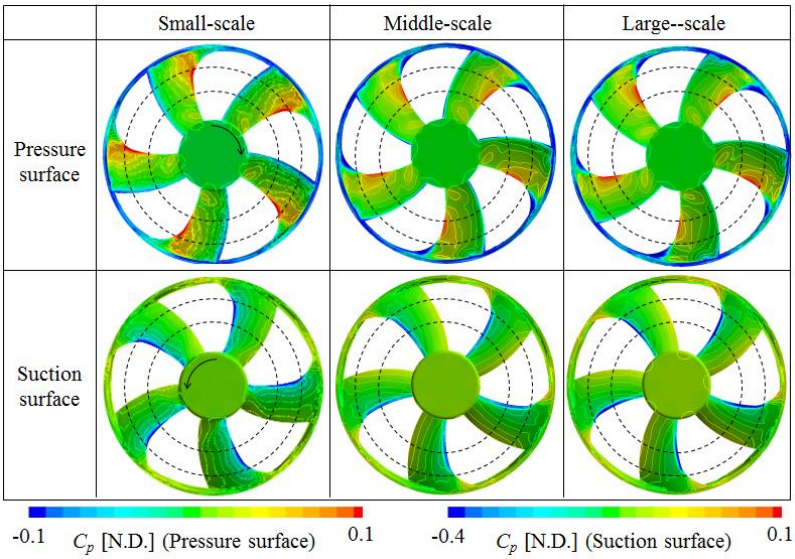

Figure 6: C_p distribution on the blade surface

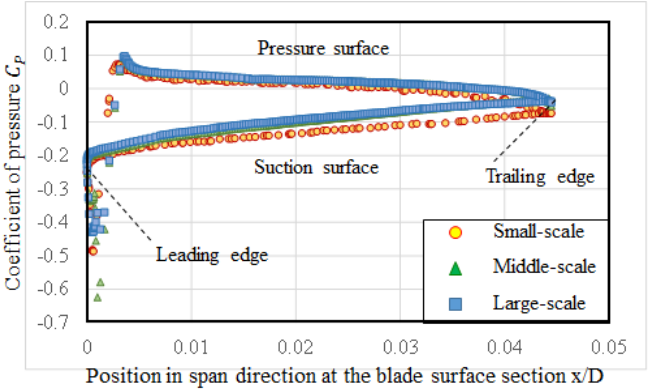

(d) C_p profile at R = 110 mm section on the blade surface

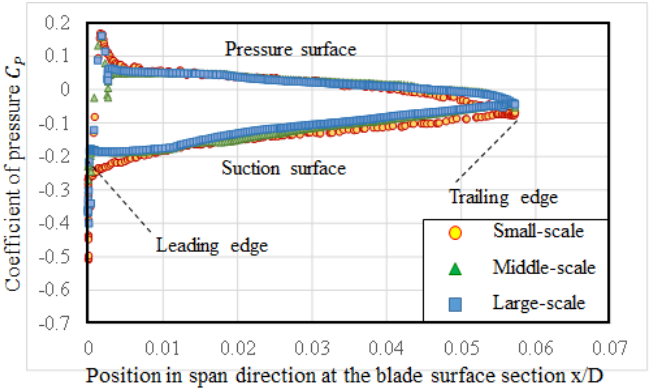

(e) C_p profile at R = 150 mm section on the blade surface

Figure 7: C_p profile at R = 110 and 150 mm on the blade surface

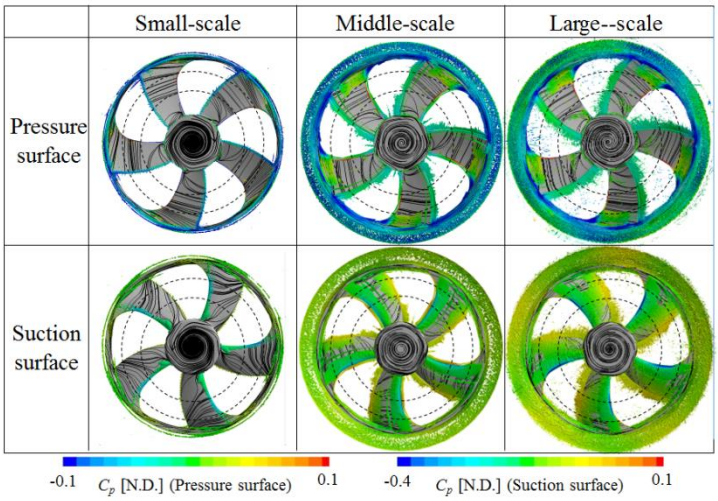

Figure 8: Isosurface of second invariance Q and streamline on the fan

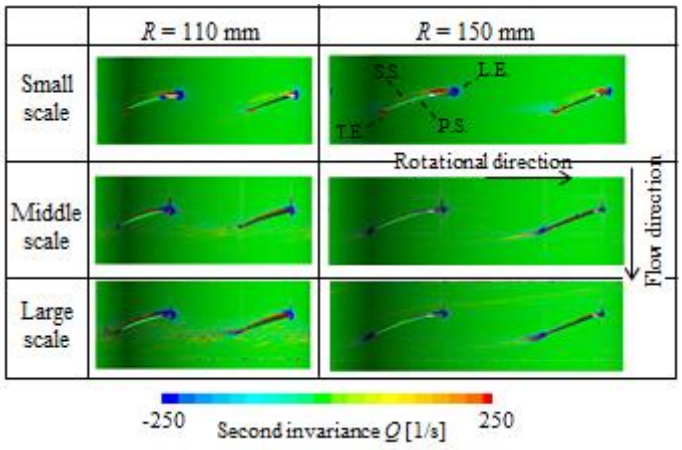

Figure 9: Q distribution at section of R = 110 and 150 mm section

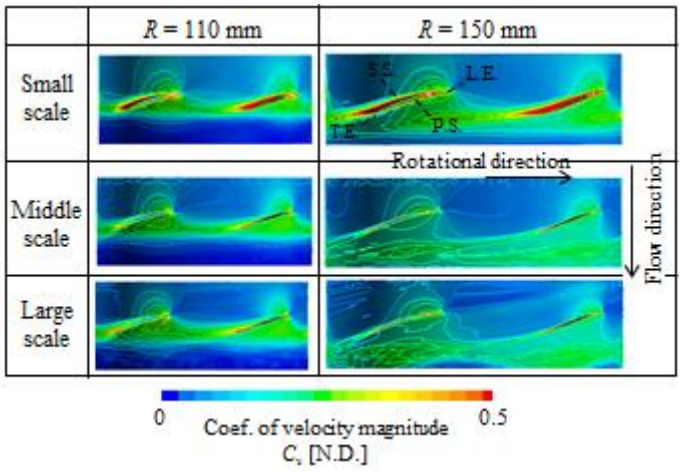

Figure 10: C_v distribution at section of R = 110 and 150 mm section

5 IMPORTANCE AND PROBLEM OF LARGE-SCALE ANALYSIS

We think that the clarification of the relationship between the fan performance and flow structures at each frequency is necessary to develop a high-performance and low-noise small cooling fan as mentioned above. For the cooling fan development, the study focused on very high-frequency region with such turbulent noise in the order of 10000 Hz and/or low-frequency region with the BPF noise for major improvement. It is difficult to study in these regions using conventional computing systems; therefore, HPCS is required. In addition, postprocessing of big data obtained from large-scale analysis remains a critical issue. In future work, we will focus on proper orthogonal decomposition (POD) [7, 8] for the analytical method of big data and classify the flow structures in each frequency to associate them with the fan performance.

6 CONCLUSIONS

The purpose of this study is to reveal the dominant flow structures on the fan performance and the essential information for the accurate prediction by conducting small-, medium-, and large-scale LES analyses using HPCS. For the case of the ring fan (such as that used in this study), it was found that accurate prediction is determined by the calculation result of the attack angle of flow because there is no large tip vortex that is absolutely generated in the case of a propeller fan. This means that the flow in boundary layer and wake structures dominate the fan performance. It should be noted that the resolution of longitudinal vortex, similar to the separation vortex, is most important when we predict the performance under the region of low flow rate conditions (region with high pressure loss condition).

REFERENCES

[1] Yuji Kobayashi et al., Influence of the Fundamental Parameters for the Blade Geometry on the Fan Performance, *Transactions of the Japan Society of Automotive Engineers, Vol.44, No.6, pp.1477-1482, November,* 2013.

[2] Kazuya Kusano et al., Three-dimensional Structures of Tip Vortex in a Half-ducted Propeller Fan, *Transactions of the Japan Society of Mechanical Engineers, Vol.80, No.810,* 2014.

[3] Tomoyoshi Sasajima et al., Numerical Analysis of Flow around Blades in Axial Flow Small Fan, *Transactions of the Japan Society of Mechanical Engineers, Series B, Vol.77, No.774, pp.255-263,* 2011.

[4] Itsuhei Kohri et al., Prediction of the Performance of the Engine Cooling Fan with CFD Simulation，*SAE International Journal Of Passenger Cars - Mechanical Systems, Vol. 7, No. 2, pp.728-738, August,* 2010.

[5] Yuji Kobayashi et al., Determination of Suitable MRF-Region for Practical Prediction of Engine Cooling Fan Performance, *AJK2011-FED, AJK2011-23005, July,* 2011.

[6] Chisachi Kato et al., Large Eddy Simulation of Unsteady Flow in a Mixed-Flow Pump : 1st Report, Numerical Method, *Transactions of the Japan Society of Mechanical Engineers, Series B, Vol.68, No.680, pp. 1729-1736,* 2002.

[7] Kunihiko Taira, Proper Orthogonal Decomposition in Fluid Flow Analysis: 1. Introduction, *Journal of Japan Society of Fluid Mechanics, Vol.30, pp.115-123,* 2011.

[8] Yuji Kobayashi et al., Proper Orthogonal Decomposition Analysis of Flow Structures Generated around Engine Cooling Fan, *SAE International Journal Of Passenger Cars - Mechanical Systems, Vol.3, Issue 1, pp.508-522, November,* 2014.